Journal of Membrane Science 685 (2023) 121915

Contents lists available at ScienceDirect

Journal of Membrane Science

journal homepage: www.elsevier.com/locate/memsci

Electrospun phosphonated poly(pentafluorostyrene) nanofibers as a reinforcement of Nafion membranes for fuel cell application

Muhammad Solihul Mu'min [a,b,1], Miriam Komma [a,b,1], Dunia Abbas [a,b], Maximilian Wagner [a], Anja Krieger [a], Simon Thiele [a,b], Thomas Böhm [a], Jochen Kerres [a,c,*]

[a] Forschungszentrum Jülich GmbH, Helmholtz Institute Erlangen-Nürnberg for Renewable Energy (IEK-11), Cauerstr. 1, 91058, Erlangen, Germany
[b] Department of Chemical and Biological Engineering, Friedrich-Alexander-Universität Erlangen-Nürnberg, Egerlandstr. 3, 91058, Erlangen, Germany
[c] Chemical Resource Beneficiation Faculty of Natural Sciences, North-West University, Potchefstroom, 2520, South Africa

ARTICLE INFO

Keywords:
Electrospinning
Phosphonated polypentafluorostyrene
Fiber-reinforced composite membrane
Fuel cell
Hydrogen crossover

ABSTRACT

Nafion is a well-known perfluorosulfonic acid membrane widely used in fuel cells. However, despite its excellent properties, Nafion has limitations, including high hydrogen crossover. Reducing the hydrogen crossover is crucial since the H_2 permeating through the membrane can directly react with O_2 and produce radicals that can degrade Nafion. The hydrogen crossover can be minimized by increasing membrane thickness or by embedding nanostructures into Nafion. In this work, we report Nafion membranes reinforced by electrospun fibers made from phosphonated polypentafluorostyrene (PWN70) and, for comparison, unmodified polypentafluorostyrene (PPFSt). Composite membranes were obtained by spray-coating of Nafion onto the nanofiber meshes to fill the voids. From tensile tests, we found that PWN70/Nafion and PPFSt/Nafion composite membranes show higher Young's modulus and higher yield stress than pure Nafion. Fuel cell tests showed that PPFSt/Nafion composite membranes suffer from performance losses with increasing fiber loading, whereas PWN70/Nafion composite membranes perform similarly with non-reinforced Nafion. Furthermore, the use of PWN70/Nafion resulted in an H_2 crossover reduction by 37–40% for atmospheric pressure, while it was not improved when using PPFSt/Nafion composite membranes. These results show the advantages of PWN70 nanofibers as a reinforcement for Nafion, which reduce the hydrogen crossover without sacrificing proton conductivity.

1. Introduction

Nafion is a standard solid polymer electrolyte used in proton exchange membrane (PEM) based electrochemical energy conversion systems, including PEM fuel cells (PEMFCs). Nafion has excellent properties, such as high protonic conductivity, and high mechanical, chemical, and thermal stability [1]. The high proton conductivity of Nafion can be traced back to the strong nanophase separation between the extremely hydrophobic perfluorinated backbone polymer nanophase and the strongly hydrophilic and proton-conducting sulfonic acid group nanophase [2]. Nevertheless, there is still room for improvement for PEMs based on Nafion to increase the fuel cells' performance and lifetime. One strategy for optimizing the performance is to decrease the ohmic resistance of the cell assembly by reducing membrane thickness [3]. However, polymer thin films based on perfluorinated sulfonic acids such as Nafion show a considerable gas crossover, and the thinner the membrane, the higher the hydrogen crossover [4]. The gas crossover through the PEM not only results in reduced faradaic efficiency, but also decreases the devices' lifetime. The direct reaction of H_2 with O_2 within the membrane-electrode assembly can produce reactive oxygen species, which degrade the polymer, resulting in membrane thinning [5]. Further, the mechanical integrity deteriorates when the membrane thickness is reduced, which eventually results in pinhole formation [6]. Therefore, Nafion can be modified in order to improve its properties. This task can be accomplished by incorporating additives such as CeO_x as a radical scavenger to mitigate chemical degradation of the membrane [7]. Alternatively, composite membranes with interlayers can be produced that reduce gas crossover, which reduces the degradation rate of the membrane by less production of reactive oxygen species [8]. Another method for improvement of the properties of perfluorinated

* Corresponding author. Forschungszentrum Jülich GmbH, Helmholtz Institute Erlangen-Nürnberg for Renewable Energy (IEK-11), Cauerstr. 1, 91058, Erlangen, Germany.
E-mail address: j.kerres@fz-juelich.de (J. Kerres).
[1] authors contributed equally to this work.

https://doi.org/10.1016/j.memsci.2023.121915
Received 11 April 2023; Received in revised form 15 June 2023; Accepted 5 July 2023
Available online 6 July 2023

sulfonic acid ionomers (PFSAs) such as Nafion is the preparation of reinforced PFSA ionomer membranes by pore-filling of porous films such as expanded PTFE (ePTFE) or PE (ePE) with the PFSA ionomer by soaking the porous films in a dispersion of the PFSA. In Ref. [9], a Nafion membrane reinforced with a microporous ePTFE foil was described, where the ePTFE surface was modified with a polydopamine (PD) layer, which served as an „interfacial glue" between the PTFE and the Nafion polymer, resulting in strong adhesion between the two polymers. Moreover, CeO_2 was added to the Nafion dispersion as a radical scavenger, which was partially reduced by the PD end groups. The resulting CeO_x nanoparticles were chemically bound to the PD interfacial layer, which diminishes CeO_2 dissolution. These membranes showed excellent long-term stability in fuel cell operation. The PD strategy for improving the adhesion between ePTFE foils and filling Nafion ionomer was also used in a study by Huo et al. [10]. After preparation of the reinforced Nafion/PD@PTFE membrane, it was treated with a DMF solution of the natural antioxidant *trans*-resveratrol as a radical scavenger. The *trans*--resveratrol-doped reinforced Nafion membranes showed a 4-fold lower hydrogen crossover than the non-treated membrane, leading to improved durability in the fuel cell test.

Electrospinning is a common method for the manufacturing of polymeric nanofibers. It harbors the option to process various polymer types and offers the option to adjust the parameters of the resulting fiber mesh, like fiber diameter, density, and even surface modifications or core-shell fiber geometries [11]. Typically, electrospun nanofibers are embedded into the membrane as mechanical reinforcement [12]. Several types of polymeric nanofibers were already used for producing composite membranes, for example PVA [13], PVDF-HFP [14], PSU [15], PBI [16], and PAN [17]. Composite membranes made of non-conductive polymer fibers embedded in an ion-conducting matrix offer a trade-off between ionic conductivity and mechanical properties [13]. A strategy to further improve composite membrane properties is to reinforce a proton-conducting membrane with proton-conductive fiber mats, ideally leading to improved mechanical properties without sacrificing ionic conductivity [18–20].

Proton-conducting nanofibers can either be selected from sulfonated and/or phosphonated polymers. There are several reports of sulfonated polymers that have been processed by electrospinning for the application as a reinforcement or as a freestanding membrane. For example, membranes produced from electrospun sulfonated poly(ether ether ketone ketone) (SPEEKK) nanofibers showed a better nanophase separation between the hydrophobic backbone and the ion-conducting channels than membranes prepared by solution-casting [21]. Another approach was the impregnation of an electrospun sulfonated poly arylene ether sulfone (SPAES) fiber mesh with an inert polymer. It was found that the resulting membranes exhibited better ultimate tensile strength and much lower O_2 permeability compared to Nafion 117 [22]. Furthermore, thin Nafion composite membranes reinforced with an electrospun nanofiber mat made from sPEK were used in a PEMFC and yielded higher peak power densities than a composite membrane with non-conductive reinforcement [20].

An alternative to sulfonated polymers is phosphonated polymers. The advantage of the phosphonic acid group is that it is proton-conductive under anhydrous conditions, whereas sulfonated polymers require a sufficient hydration [23,24]. While several studies have been conducted on the preparation of composite membranes reinforced with electrospun sulfonated nanofiber mats, composite membranes containing phosphonated polymer nanofiber mats have not been reported yet. Phosphonated poly(pentafluorostyrene) (PPFSt) or poly(2,3,5,6-tetrafluorostyrene-4-phosphonic acid), abbreviated in the following as PWN [25], is one of the most promising phosphonated polymers for fuel cells. It possesses an acidity that is significantly higher than that of polystyrene-4-phosphonic acid due to its strongly electron-attracting F substituents (the pK_a value of poly(2,3,5,6-tetrafluorostyrene-4-phosphonic acid) is ~0, while the pK_a value of poly(styrene-4-phosphonic acid is ~2). Further, PWN can be synthesized with different phosphonation levels [26,27] to tailor the hydrophobicity of the material according to its desired application.

PWN shares similar structural features to Nafion, with its aliphatic, hydrophobic main chain and the acidic side chain, and actually, it was found that the proton conductivity of PWN is high, both in hydrated and dry conditions [28]. In Fig. 1, the structural formulas of PPFSt and PWN70, respectively, are shown.

Thus, PWN is a promising material to form composites with Nafion. Pure PWN is too brittle to form stable membranes, but a reinforcement layer made from this material may improve the mechanical properties of a composite membrane. At the same time, the interactions between the SO_3H groups of Nafion and the PO_3H_2 groups of PWN can support the interfacing between the two polymers and assist in proton conduction.

Here, electrospun nanofibers from PWN70 (PPFSt with a phosphonation degree of 70%) and non-phosphonated PPFSt were prepared and incorporated into Nafion to form composite membranes. The mechanical and morphological features of these composite membranes were evaluated by scanning electron microscopy (SEM), tensile testing, and confocal Raman microscopy. Further, the performance of the composite membranes was analyzed in a low-temperature PEMFC.

2. Experimental

2.1. Materials

Potassium persulfate (99+ % for analysis) and sodium phosphate (monobasic, 99%) were used from Acros Organics. Sodium dodecyl sulfate was purchased from VWR. N,N-dimethylacetamide (DMAc; anhydrous, 99.8%), dimethyl sulfoxide (DMSO), tetrahydrofuran (THF), and isopropanol (99.8% (GC)) were purchased from Sigma Aldrich. Tris (trimethylsilyl)phosphite (95%) and pentafluorostyrene (98%) were purchased from Manchester Organics. All chemicals were used without further purification. The catalyst consisting of Vulcan XC-72 with 40 wt % platinum nanoparticles (TEC10V40E) was ordered from Tanaka and used on both electrodes. Nafion dispersion (D2020 and D2021) was purchased from Ion Power.

2.2. Polymer synthesis

2.2.1. Polypentafluorostyrene (PPFSt) synthesis

The synthesis of PPFSt was carried out according to the literature [29]. Sodium dodecyl sulfate (2.5 g, 8.6 mmol) and monosodium phosphate (0.125 g, 1.1 mmol) were dissolved in degassed water (250 ml). Potassium peroxydisulfate (0.55 g, 2.3 mmol) was added and stirred until completely dissolved. Pentafluorostyrene (125 g, 0.64 mol) was added at vigorous stirring leading to a homogeneous emulsion. The emulsion was filled into microwave vessels, and the reaction was executed in the microwave at a constant temperature of T = 90 °C for 2 h. The mixture was precipitated in an isopropanol water mixture (1:1 v/v). The solid was filtered, washed with isopropanol and water, and

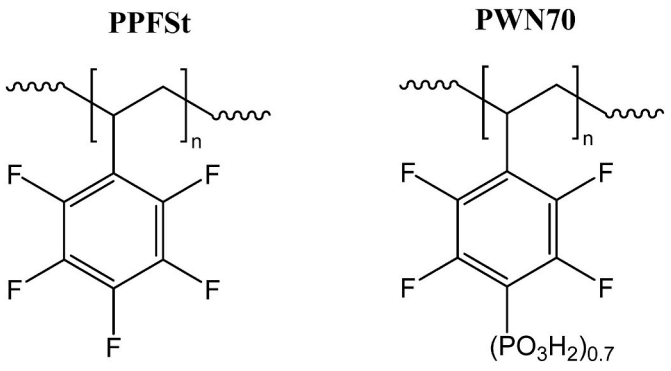

Fig. 1. Structural formulas of PPFSt and PWN70.

dried in a vacuum at 80 °C for two days. The yield (white powder) was 110 g (88%). ^{1}H and ^{19}F NMR spectra were collected at room temperature on a 500 MHz JEOL JNM-ECZR spectrometer equipped with a ROYALPROBE HFX. Molecular weight and molecular weight distribution of PPFSt were measured in THF using an Agilent GPC/SEC with polystyrene standards.

^{1}H NMR (in d8-THF): δ = 2 ppm, 2.5 ppm, 2.8 ppm

^{19}F NMR (in d8-THF): δ = −144 ppm, −158 ppm, −165 ppm

GPC: M_n = 174 kDa, M_w = 334 kDa

2.2.2. Phosphonated polypentafluorostyrene (PWN70) synthesis

The synthesis of PWN was performed related to the literature [25,26]. The previously synthesized PPFSt (50 g, 0.28 mol monomer units, molecular weight M_n = 174 kDa, M_w = 334 kDa) was dispersed in N, N-dimethylacetamide (200 ml) under argon. For phosphonation, fresh tris(trimethylsilyl)phosphite (TMSP) (70 ml, 63 g, 0.21 mol) was added.

The reaction solution was then heated to 170 °C for 10 h. After the reaction, the warm mixture was quenched with 100 ml of water. The resulting white powder was refluxed in 1 l de-ionized water two times for 30 min each, exchanging water each time. Next, the powder was boiled in a 5 wt% HCl solution and refluxed in 2.5 l de-ionized water. Finally, the polymer chunks were dried in the oven at 85 °C for two days. The yield was 63 g (96%).

^{1}H NMR (in DMSO-d_6): δ = 1.9 ppm, 2.4 ppm, 2.9 ppm

^{19}F NMR (in DMSO-d_6): δ = −135 ppm, −144 ppm, −158 ppm, −165 ppm

The degree of phosphonation was controlled with ^{19}F NMR by integration of the peak at $\delta = -135$ ppm (equals two fluorine atoms from phosphonated PPFSt) and $\delta = -165$ ppm (equals two fluorine atoms from PPFSt). The phosphonation degree was obtained by calculating the ratio of these peaks and was determined as 66%. This polymer is referred to as PWN70 in the following.

2.3. Composite membrane fabrication

The fiber-reinforced composite membranes were prepared in several steps, as illustrated in Fig. 2. For spray-coating, Nafion dispersion (D2020) was diluted to 2.5 wt% with isopropanol and homogenized using a Vortex device. The first Nafion layer was produced by an ExactaCoat ultrasonic spray-coating device (Sono-Tek, USA) onto an inert plastic substrate. Spray-coating was performed with 9 runs at a flow rate of 0.8 mL min^{-1}, nozzle speed of 100 mm s^{-1}, shaping air of 0.2 kPa, ultrasonic power of 3 W, and plate temperature of 25 °C. Separately, the reinforcement layers were produced by an electrospinner (KATO TECH CO., LTD., Japan) on an aluminum substrate. Electrospinning solutions were prepared for PWN70 (14 wt% dissolved in DMSO) and PPFSt (14 wt% dissolved in THF/DMAc (1:1)). PWN70 was spun at 20 kV with a flow rate of 2 mL h^{-1}. PPFSt fibers were produced at 10 kV and with 3 mL h^{-1}. Each polymer solution was loaded into a 20 ml syringe connected with a 21 G metallic needle. The distance between the tip of the needle and the aluminum collector was 15 cm. For the PWN solution, electrospinning was conducted at a chamber temperature of 33–34 °C to increase the evaporation rate of DMSO by using a custom-built pre-chamber that heated the inlet air. Meanwhile, electrospinning of PPFSt was performed at room temperature (T = 23.5 ± 0.5 °C, rH = 47 ± 2%). The diameter of the electrospun fibers was measured in ImageJ. The electrospun fiber mat was peeled off from aluminum substrate, and the area density was determined by weighing 2 × 2 cm^2 of the fiber mat. The peeled off fiber mat with a size of 9 × 25 cm^2 was transferred onto the first Nafion layer and then infiltrated with Nafion during the second spray-coating step. For a good infiltration of the fiber mat, the first two runs were performed at a nozzle speed of 150 mm s^{-1} and a flow rate of 0.5 mL min^{-1}. Subsequently, 10 runs were conducted with the same parameters as the first Nafion layer. The resulting composite membrane comprised three layers (Nafion - fiber mat impregnated with Nafion - Nafion). Spraycoated Nafion without

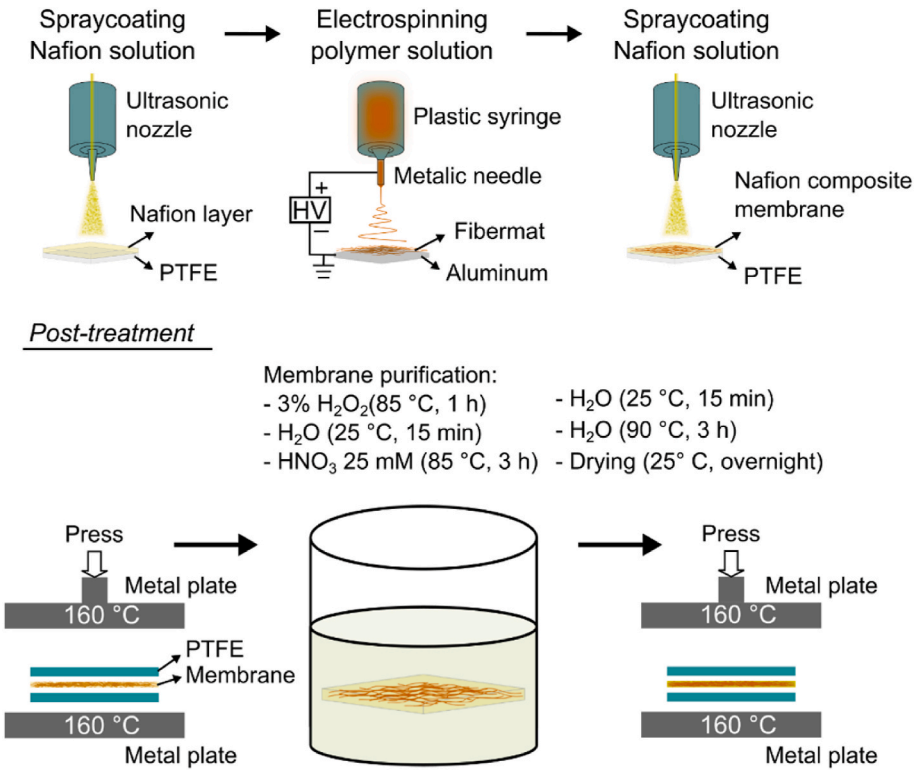

Fig. 2. Preparation of Nafion membranes reinforced by electrospun nanofibers.

reinforcement was produced as a reference by spraying the Nafion dispersion with the parameters of the first Nafion layer of the composite membranes but with 25 runs to get one continuous layer of Nafion.

A first hotpressing step (160 °C, 5 min, 2 MPa) was performed on the membranes to improve the interface between the membrane matrix and fiber reinforcement. Next, the membranes were treated to remove residual solvents. First, they were immersed in 3% H_2O_2 at 85 °C for 1 h and then transferred into de-ionized water for 15 min. In the second step, the membranes were incubated in 25 mM HNO_3 at 85 °C for 3 h, followed by immersion in de-ionized water for 15 min. Finally, the membranes were incubated in de-ionized water at 90 °C for 3 h and dried overnight at room temperature. The membranes were hotpressed (160 °C, 5 min, 2 MPa) a second time to improve the membranes' mechanical properties and get rid of wrinkles.

2.4. Ex situ membrane characterization

2.4.1. Scanning electron microscopy

Electrospun nanofiber meshes and cross-sections of MEAs were investigated using scanning electron microscopy (SEM). A sample of the fiber mat was taken using a scalpel and put onto an aluminum specimen stub using double-sided adhesive carbon tape. Cross-sections of the MEAs were prepared after fuel cell testing by embedding pieces of the catalyst-coated membranes CCMs in epoxy resin after removal of the GDLs. The cross-sections were prepared using ultramicrotomy (RMC Boeckeler PowerTome XL) with a Diatome diamond knife and fixed in aluminum specimen stubs. The samples were sputter-coated with gold prior to imaging. Imaging was performed on a Tescan Vega 3 at an acceleration voltage of 15 kV.

2.4.2. Tensile testing

The membranes' mechanical properties were measured using a tensile tester (EZ-SX, SHIMADZU Corporation, Japan) at room temperature (T = 23.5 ± 0.5 °C, rH = 47 ± 2%). The thicknesses of the membranes were measured by a micrometer gauge and were comparable between 30 and 34 μm. Before the measurement, all membranes were cut into a rectangular shape with an area of 1 cm × 5 cm. The membrane samples were assembled in the device and were stretched in the longitudinal direction with a constant speed of 5 mm min^{-1}. Based on the resulting stress-strain curve, the Young's modulus was determined from the slope in the elastic region using the equation

$$E = \Delta\sigma/\Delta\varepsilon \quad (1)$$

where σ and ε are stress and strain, respectively, and E is the Young's modulus. The elastic limit is indicated by the yield stress, which was determined by choosing 0.5% strain offset for membranes with reinforcement and 1% for the reference membrane since it is without fiber support [30]. Three samples were measured per membrane type and the mean of these measurements was used as a result.

2.4.3. Confocal Raman microscopy

The membranes were analyzed with confocal Raman microscopy (WITec alpha 300) to investigate the fiber mat position and hydrophilicity within the membranes non-destructively. A water immersion objective (Zeiss W Plan Apochromat 63x/1) was used with a custom sample holder that enabled through-plane imaging of the membranes with water below and above the sample [31]. The microscope was operated with a 532 nm laser at 50 mW excitation power and recorded spectra with a Peltier-cooled EMCCD camera (WITec UHTS300 Vis). Confocal through-plane scans were recorded with a pixel size of 400 nm (overview images) and 200 nm (detailed images of the reinforcement layers) with an integration time of 0.1 s $pixel^{-1}$. The evaluation of the hyperspectral images was conducted analogously to Ref. [32]. In brief, reference spectra of all materials were recorded separately (water, Nafion, PWN70, and PPFSt) and used to create false-color images of the through-plane scans using a custom-built multivariate algorithm. First, the background of all spectra was subtracted using the shape-based algorithm in WITec Project 5+. All further processing steps were performed with Matlab. The data was analyzed within the spectral interval from 200 to 3800 cm^{-1}, and the reference spectra were prepared by setting the reference spectrum of Nafion to the baseline at >1500 cm^{-1}. This step was needed to obtain a Nafion reference without the OH-related bending and stretching vibrations at around 1620 and 3450 cm^{-1}, which enabled an analysis of the spectral ratio between Nafion and water in composites to evaluate the hydrophilicity of the fibers. Then, the set of reference spectra was fitted to the hyperspectral through-plane images using a least squares approach, which resulted in a spectral contribution factor for each of the references at all pixels of the images. This data was converted into false-color-coded images and scaled up for graphical representation using bicubic filtering.

2.5. Membrane electrode assembly preparation and fuel cell testing

Decal electrodes were manufactured from an ink containing 0.58 g commercial Pt/C catalyst (TEC10V40E), 1.07 g Nafion D2021 dispersion, 4.02 g 1-propanol, and 0.26 g water. ZrO_2 beads were added as a grinding medium, and the ink was mixed on a roller mill for 24 h at 60 rpm. The electrode ink was cast onto PTFE substrate sheets using the Mayer rod technique with a 100 μm rod. Afterward, the electrodes were dried at 70 °C for 1 h. Electrodes with an active area of 5 cm^2 were cut from the electrode sheets and hotpressed (1st Step: 120 °C, 1 min, 0.5 MPa; followed by a temperature and pressure ramp within 2.5 min to the 2nd Step: 155 °C, 4 min, 2.5 MPa) onto the membranes to form catalyst-coated membranes (CCMs). The electrode loading was determined by the weight difference of the PTFE substrates with and without the catalyst layer. The electrode loadings were determined as 0.22 ± 0.03 mg_{Pt} cm^{-1} for the anodes and 0.32 ± 0.02 mg_{Pt} cm^{-1} for the cathodes. The CCMs were assembled with gas diffusion layers (GDLs) from Freudenberg (H23C8) to form membrane electrode assemblies (MEAs).

For every membrane type, 3 MEAs were assembled in a 5 cm^2 PEMFC cell fixture of Scribner Associates Inc., which consists of aluminum end plates, gold-plated copper current collectors, and serpentine-patterned graphite flow fields. The fuel cell was tightened with 5 Nm torque, and a compression of 20% was adjusted by glass fiber-reinforced PTFE gaskets. The MEAs were tested using a Scribner 850e fuel cell system at 80 °C cell temperature, atmospheric pressure, fixed flow rates of 0.25 l min^{-1} H_2 and 0.75 l min^{-1} air, and 95% relative humidity. The break-in was conducted with the Scribner fuel cell system and consisted of 3 repetitions, each holding 0.6 V for 25 min, followed by 5 min open circuit voltage (OCV), and 5 min holding 0.3 V. After the break-in, galvanostatic polarization curves were recorded using a VSP-300 potentiostat (Biologic SAS), with a hold time of 5 min at each current density, each followed by impedance measurements (200 kHz–1 Hz). Linear sweep voltammetry (LSV) was performed for the determination of the H_2 crossover after 1 h of purging the cathode compartment with 1 l min^{-1} N_2 at 95% relative humidity. LSV scans were conducted from the onset potential 0 V vs. OCV to 0.6 V vs. reference at a scan rate of 2 mV s^{-1}. The anode compartment of the fuel cell was fed with 0.2 l min^{-1} H_2, and the cathode compartment with 0.2 l min^{-1} N_2. Before every LSV scan, an impedance scan with a frequency range from 100 kHz to 10 Hz at those blocking conditions was recorded. After collecting the LSV data at atmospheric pressure, the same LSV measurements were performed additionally at 1.5 bar absolute balanced pressure. LSV and impedance measurements were conducted using the VSP-300 potentiostat.

Polarization curves were corrected for the high-frequency resistance (HFR) of the MEAs by correcting the cell potential E_{cell} [V] with the HFR [mΩ cm^2] and the current density I [mA cm^{-2}] according to Equation (2).

$$E_{corrected} = E_{cell} + I \bullet HFR \quad (2)$$

All LSV measurements were corrected for the individual electrical

short resistance of the MEAs according to Equation (3), where $I_{H_2\ crossover}$ [mA cm^{-2}] is the hydrogen crossover current density from the LSV measurement. $E_{LSV(onset)}$ [V] and $E_{LSV(n)}$ [V] equal the cell potential while sweeping from the onset potential to the potential in step n, and R_{short} [mΩ cm^2] is the electrical short resistance of the MEA (derived from the slope of the LSV measurement).

$$I^{corr}_{H_2\ crossover} = I_{H_2\ crossover} - \left(E_{LSV(n)} - E_{LSV(onset)}\right) \bullet R^{-1}_{short} \quad (3)$$

For the calculation of the Tafel slopes, E_{cell} was corrected for the corrected H_2 crossover current $I^{corr}_{H_2\ crossover}$ [mA cm^{-2}], the electronic short resistance of the MEA R_{short} [mΩ cm^2], both obtained from LSV data at atmospheric pressure, the HFR [mΩ cm^2], and the effective proton conduction resistance ($R^{eff}_{H^+,cath}$ [mΩ cm^2]), each determined by impedance analysis at atmospheric pressure, as shown in Equations (4)–(6) [33].

$$E_{corrected} = E_{cell} + I \bullet \left(HFR + R^{eff}_{H^+,cath}\right) \quad (4)$$

$$\text{With } R^{eff}_{H^+,cath} = R_{H^+,cath} \Big/ 3 \quad (5)$$

$$I_{corrected} = I + I^{corr}_{H_2\ crossover} + E_{cell} \bullet R^{-1}_{short} \quad (6)$$

HFR values were determined by fitting the acquired impedance data, which were recorded after every hold in the polarization curve, with the equivalent circuit according to Baker et al. containing an inductor L, resistor R and a transmission line model for H_2/O_2 operation [34]. The fitting was performed using impedance.py for Python.

The proton conduction resistance $R_{H^+,cath}$ was determined from the impedance data measured at blocking conditions (H_2/N_2). The applied equivalent circuit consisted of an inductor L_a for the cell inductance, a resistor R for the HFR, and a restricted linear diffusion element M_a for the proton conduction resistance. The fitting process was conducted with the software "Z-fit" from Biologic SAS. The effective proton conduction resistance $R^{eff}_{H^+,cath}$ was determined according to Neyerlin et al. as it can be seen in equation (5) [33].

3. Results and discussion

3.1. Electrospinning of PPFSt and PWN70

The PWN70 nanofibers were spun from a high boiling point solvent (DMSO), making it challenging to evaporate during electrospinning at room temperature. A considerable amount of solvent was still left in the nanofibers upon deposition on the collector. Thus, the wet nanofibers tended to fuse with adjacent nanofibers, which caused nanofiber morphology to be less homogeneous (Fig. 3A and B). In addition, the leakage current during electrospinning frequently fluctuated from 30 to 50 μA and even up to 70 μA when the process was maintained for a more extended period, indicating that the polymer stream coming out of the needle was unstable. As shown in Fig. 3C and D, homogeneous PWN70 nanofibers with diameters of 500–800 nm were produced when the chamber temperature was increased to 32–34 °C. The electrospinning of PPFSt was conducted at room temperature (T = 23.5 ± 0.5 °C, rH = 47 ± 2%), which was likely enabled by the solvents of this polymer solution that had lower boiling points. The electrospun PPFSt fibers display a diameter above 2–6 μm (Fig. 3E and F), which is significantly higher than the diameter of the PWN70 nanofibers. The significant dissimilarity between PPFSt and PWN70 fiber diameters can be attributed to the fact that PPFSt does not contain ion-exchange groups and is therefore not proton-conductive, in contrast to PWN70 which shows a good proton conductivity. Conductivity is one of the electrospinning parameters that can generate substantial fiber elongation during electrospinning [35]. A polymer solution with high ionic conductivity contains a lot of electrical charges that promote stretching of the polymer jet under an electric field. This elongation process contributes to the thinning of fiber diameter.

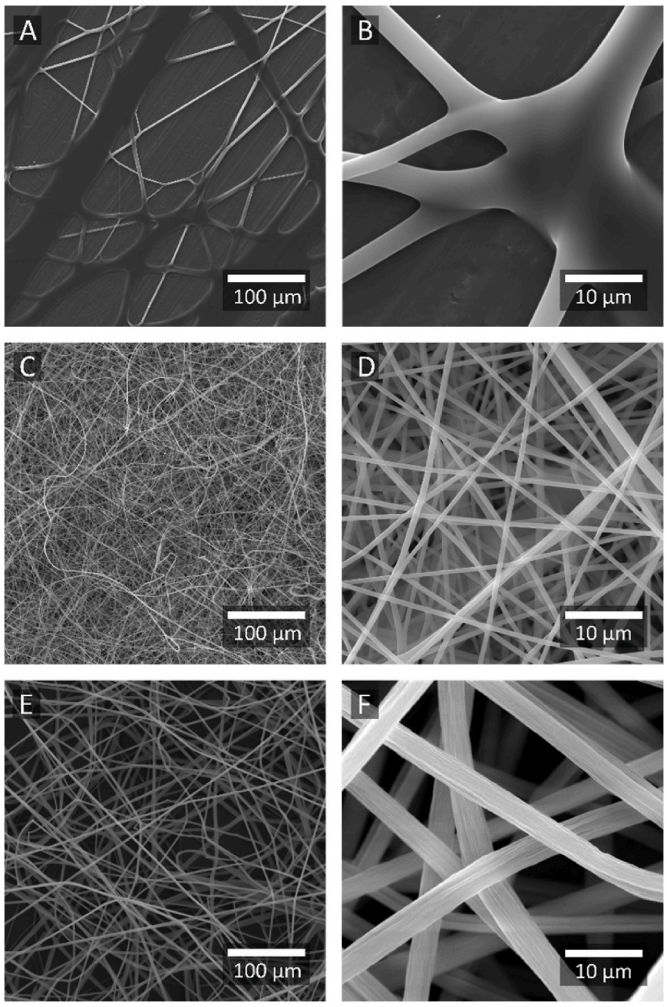

Fig. 3. SEM images of PWN70 nanofibers produced at room temperature (T = 23.5 ± 0.5 °C, rH = 47 ± 2%) (A and B), at 33 °C ± 1 °C (C and D), and PPFSt fibers produced at room temperature (T = 23.5 ± 0.5 °C, rH = 47 ± 2%) (E and F).

3.2. Mechanical and morphological properties of composite membranes

The mechanical properties of fiber-reinforced composite membranes are governed by the fiber material, the fiber loading (area density), and the fiber-matrix interface. On the one hand, the nanofiber loading needs to be sufficiently high to improve the mechanical properties. On the other hand, composite membranes with too high fiber loadings can suffer from performance losses due to impaired proton conductivity or poor infiltration of the fiber mesh with the matrix polymer. In Fig. 4A and C, dense electrospun fiber mats with a loading of 1 mg cm^{-2} are depicted. After hotpressing, the fiber-reinforced Nafion membrane was transparent (Fig. 4B and D), indicating that the fiber mat was successfully filled with the matrix ionomer Nafion [36]. Hotpressing is a simple but effective way to accomplish an improved fiber-matrix interface for Nafion-based composite membranes. Since Nafion is thermoplastic, hotpressing above its glass transition temperature, which is around 120 °C [37], makes the polymer chains flexible to penetrate the voids within the fiber mats. Further, thermal annealing can also increase the degree of crystallinity of Nafion and thereby enhance the mechanical properties [38]. The lack of transparency compared with PWN70 reinforced Nafion prior to hotpressing indicates a poor infiltration of the

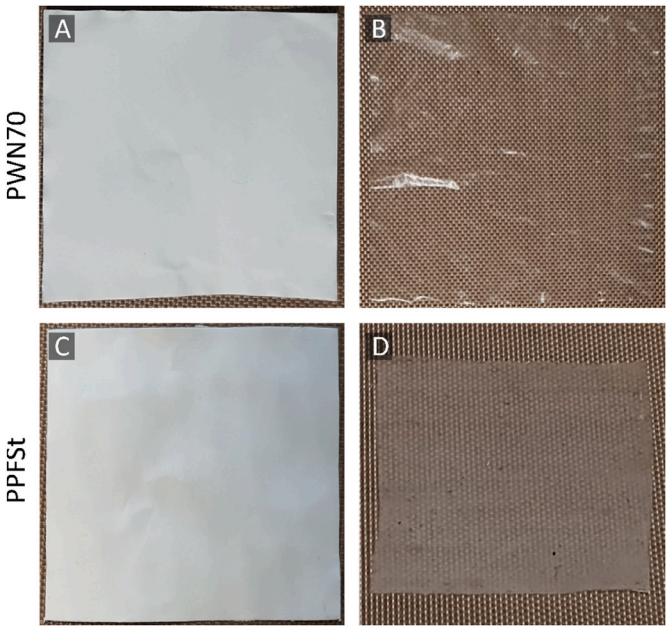

Fig. 4. Photograph of the PWN70 (top) and PPFSt (bottom) fibermat with a density of 1 mg cm^{-2} before (A, C) and after (B, D) the incorporation into Nafion to form composite membranes.

fiber mat. This behavior might be attributed to the bad compatibility between the purely hydrophobic PPFSt and Nafion with its hydrophobic and hydrophilic domains. After hotpressing, the PPFSt/Nafion composite membrane turns from opaque to transparent (compare Figure S1 and Fig. 4D). This observation validates the need for hotpressing to improve the interfacial adhesion between fibers and matrix. In Fig. 5, cross-sections of the composite membranes after fuel cell testing are presented. The CCMs were embedded in epoxy resin, and the cross-sections encompass the (composite) membrane and the catalyst layers. Fig. 5A presents the cross-section of the reference CCM, which contains a non-reinforced homogeneous Nafion membrane. In the PWN70/Nafion composite membranes (Fig. 5B and C) with 0.5 and 1.0 mg cm^{-2}, the appearance of a darker layer indicates the PWN70 nanofibers. The PWN70 nanofibers are strongly attached with Nafion due to their ability to create hydrogen bonding between sulfonic and phosphonic acid groups [39]. In contrast, the PPFSt fibers with 0.5 and 1.0 mg cm^{-2} (Fig. 5D and E) are not fully attached to the surrounding Nafion matrix, resulting in voids that can be observed as black rims surrounding the fibers. This detachment of the fibers is likely an artifact from sample processing for obtaining the cross-sections, which involved physical sectioning using ultramicrotomy. The forces acting on the sample during sectioning in concert with the different mechanical properties of fibers and matrix can result in a detachment. This phenomenon did not occur in the PWN70-reinforced membranes, which can be explained by the better interface between PWN70 and Nafion compared with PPFSt and Nafion. The PWN70 fiber reinforcement is located in the center of the membrane, as it was intended by the 3-step manufacturing process. On the other hand, the PPFSt fibers, especially at the higher area density, are closer to one of the electrodes. This finding can be explained by the larger fiber diameter of the PPFSt fibers, which leads to a less compact mesh. Nonetheless, good infiltration can be observed for all composite membranes since no voids can be observed in the PWN70 reinforced composite membranes and the Nafion layers are fully interconnected through the reinforcement of the PPFSt reinforcement, which renders these membranes suitable for PEMFC application.

Confocal Raman microscopy was performed in addition to electron microscopy to investigate the morphology of the fiber structure within the composite membranes. The cross-sections in Fig. 6 were obtained optically without physically cutting the sample since confocal microscopy is a non-destructive analysis method. The overview images of the membranes in Fig. 6A–C shows that the infiltration of the fibers was successful: There is no evidence of entrapped air or water in voids surrounding the fibers, which confirms the hypothesis that the fiber detachment of PPFSt fibers in Nafion in Fig. 5D and E stems from the sample preparation for electron microscopy. However, it can be noted that the image quality in Fig. 6C deteriorates significantly below the fibers, which is observable as a blurring between the different phases within the image. This phenomenon is an optical artifact that occurs in through-plane confocal microscopy due to the mismatch in refractive indices between the immersion medium (water) and the polymer fibers [40,41]. The artifact is pronounced in the Raman image of the

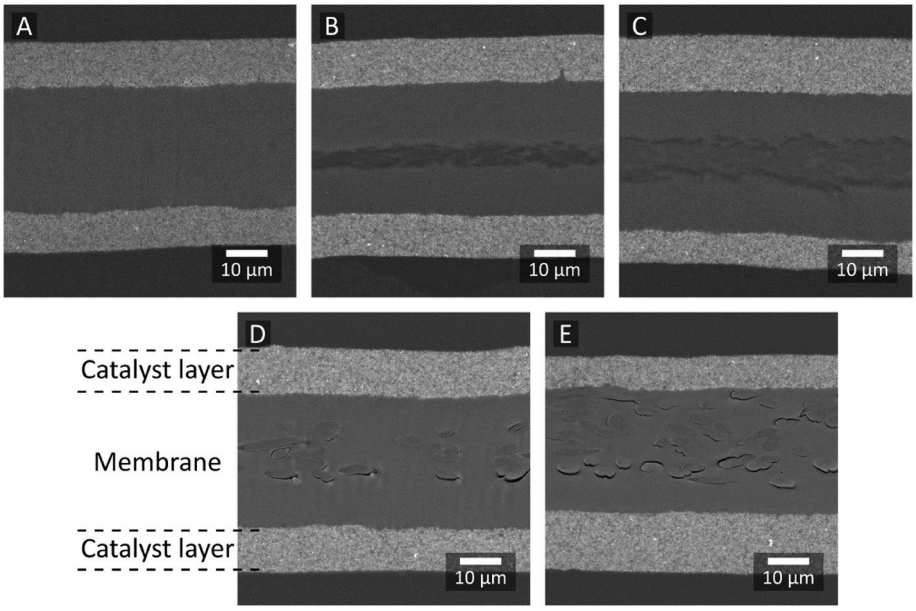

Fig. 5. Cross-sectional electron micrographs of membrane electrode assemblies with reference membrane (A), composite membrane with 0.5 mg cm^{-2} PWN70 fibers (B), composite membrane with 1 mg cm^{-2} PWN70 fibers (C), composite membrane with 0.5 mg cm^{-2} PPFSt fibers (D), and composite membrane with 1 mg cm^{-2} PPFSt fibers (E).

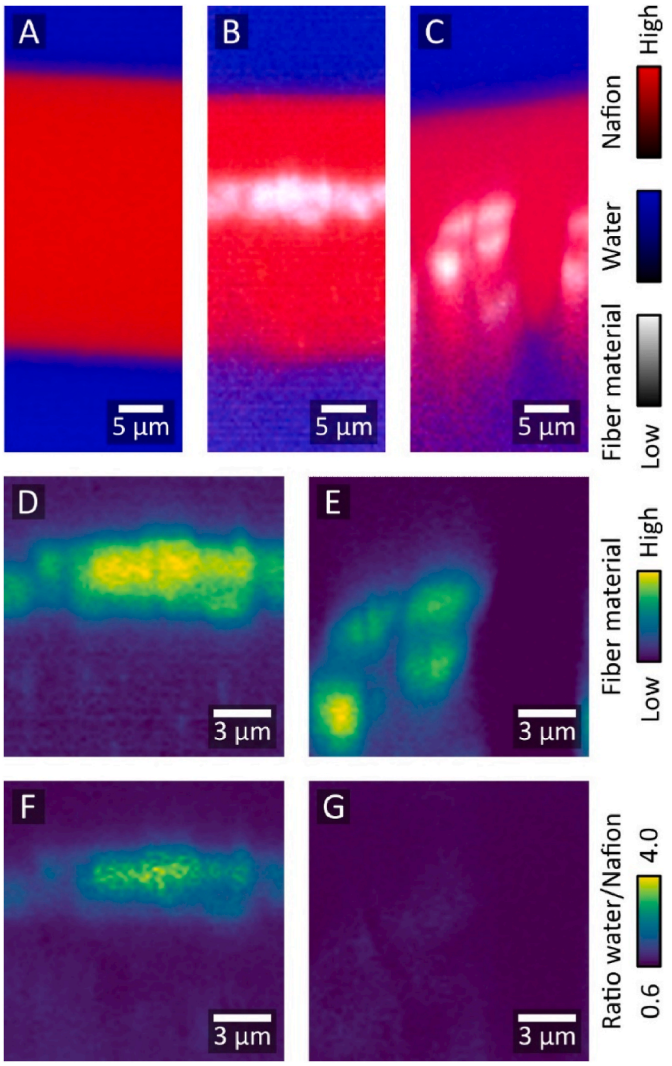

Fig. 6. Raman images of membranes. Provided are optical cross-sections of water-immersed membrane samples. The upper row shows overview images of the different membranes with plain Nafion (A), Nafion with 0.5 mg cm^{-2} PWN70 nanofibers (B), and Nafion with 0.5 mg cm^{-2} PPFSt nanofibers (C). Note that the blurring below the fiber mesh in the composite membranes is an optical artifact originating from through-plane imaging. The center row shows high-resolution images of the fiber-reinforced membranes in the upper row. D), Nafion with 0.5 mg cm^{-2} PWN70 fibers, and E), Nafion with 0.5 mg cm^{-2} PPFSt fibers. The bottom row shows the same field of view as the center row but the spectral intensity ratio of water to Nafion. Increased intensities in F) denote the hydrophilicity of PWN70, whereas the homogeneous ratio of water to Nafion in G) shows that PPFSt does not absorb water.

PPFSt-reinforced Nafion membrane, which may be caused by the larger diameter of the fibers compared to the PWN70-reinforced Nafion membrane (compare Fig. 3). The high-resolution images in Fig. 6D and E confirm the different fiber diameters of the two reinforcement layers because the PWN70 fibers are too small to be individually resolvable using confocal microscopy. In contrast, single fibers can be identified in the reinforcement layer of the PPFSt-Nafion composite membrane. The same data was used to determine the hydrophilicity of the reinforcement layers qualitatively. From the hyperspectral Raman images, the ratio of the spectral contributions of water and the matrix polymer Nafion was extracted and is displayed in Fig. 6F and G, with an increased ratio equalling a higher intensity. In these images, the baseline intensity in the Nafion matrix corresponds to the water uptake of Nafion. However, at the position of the fiber reinforcement, there is less matrix polymer sampled per pixel due to the limited spatial resolution of confocal microscopy (axial resolution approximately 1.6 µm [31]). Thus, the single pixels equal a sampling volume that includes the fiber material and the surrounding matrix. Consequently, a hydrophobic fiber material does not alter the detected ratio between water and Nafion, whereas a hydrophilic fiber material results in an increased water/Nafion ratio. This pattern is reflected by the two fiber-reinforced membranes, with phosphonated PWN70-reinforced Nafion showing a higher water/-Nafion ratio at the positions of the fibers but no change in the water/-Nafion ratio for the hydrophobic PPFSt-reinforcement in Nafion. Thus, PWN70 fibers harbor the potential to provide a functional advantage to the composite membrane by contributing to the necessary water uptake for proton conduction besides acting as a mechanical reinforcement layer.

Fuel cell membranes are exposed to mechanical stresses during assembly and operation, which is especially critical for thin membranes and may cause catastrophic failure if the membrane ruptures during operation [42,43]. The membrane needs to be stiff and ductile to withstand deformation and ultimately failure under load. The stiffness of the membrane is represented by a high elastic performance (high Young's modulus and high yield strength), while a high elongation at break indicates a ductility. Embedding a fiber reinforcement into a PFSA membrane allows to improve the elastic strength of the membrane. The composite membranes were analyzed by tensile testing in the dry state to identify the mechanical properties (stress-strain curves of PWN70/Nafion, PPFSt/Nafion, and Nafion are provided in Fig. S2) at room temperature and ambient humidity. The Young's moduli and yield strengths of the membranes are presented in Fig. 7A and B, respectively. PPFSt and PWN70 fiber-reinforced membranes show improvements for both values compared to the Nafion reference membrane. The PWN70-reinforced membrane with a fiber loading of 0.5 mg cm^{-2} shows a Young's modulus of 387 ± 10 MPa, which is an 83% increase compared to non-reinforced Nafion. However, by further increasing the PWN70 loading to 1.0 mg cm^{-2}, the Young's modulus and the Yield strength decrease. The deterioration of the mechanical properties with higher loadings might be attributed to the higher water uptake of the hydrophilic PWN70 fiber mat from the surrounding environment, which might make the composite membrane softer. Nonetheless, the Young's modulus and yield strength of the composite membrane with 1 mg cm^{-2} PWN70 fibers are still 65% and 22% higher than the corresponding values of the reference. In addition, these results highlight the favorable properties of forming composites with nanofibrous structures: Pure PWN70 is too brittle to form mechanically stable membranes [44]. By electrospinning PWN70, fiber mats are formed that can be used to enhance the mechanical properties of a matrix polymer. In the case of PPFSt/Nafion, the mechanical properties improve with increasing loading. When the density of PPFSt fiber in the Nafion composite membrane is 0.5 mg cm^{-2}, the modulus of elasticity is 347 ± 10 MPa or increased by 64% compared to Nafion without reinforcement. Increasing the PPFSt content to 1.0 mg cm^{-2} further increased the Young's modulus by 106%. Additionally, the yield strengths of PPFSt-reinforced membranes with a fiber loading of 0.5 mg cm^{-2} and 1.0 mg cm^{-2} are 20% and 42% higher than that of Nafion, indicating that a higher fiber loading results in a higher yield strength. It can be noted that adding more PPFSt fibers mechanically strengthens the composite membrane, whereas the composite membrane with PWN70 did not profit from higher fiber loadings. This finding can be traced back to the nonpolar and highly hydrophobic PPFSt fibers, which do not take up water, whereas it can be hypothesized that PWN-reinforced membranes may show deviating results due to the water uptake of the reinforcement. Therefore, the higher the PPFSt fiber loading, the higher the PPFSt/Nafion yield strength. On the other hand, for PWN70 fiber-based reinforcements, there may be an ideal compromise between the fiber loading and a beneficial effect on the mechanical properties, which likely depends on the expected humidity during operation of the composite membrane. Further, dynamic-mechanical analysis (DMA) was performed at 80 °C in dry and wet conditions to measure the mechanical

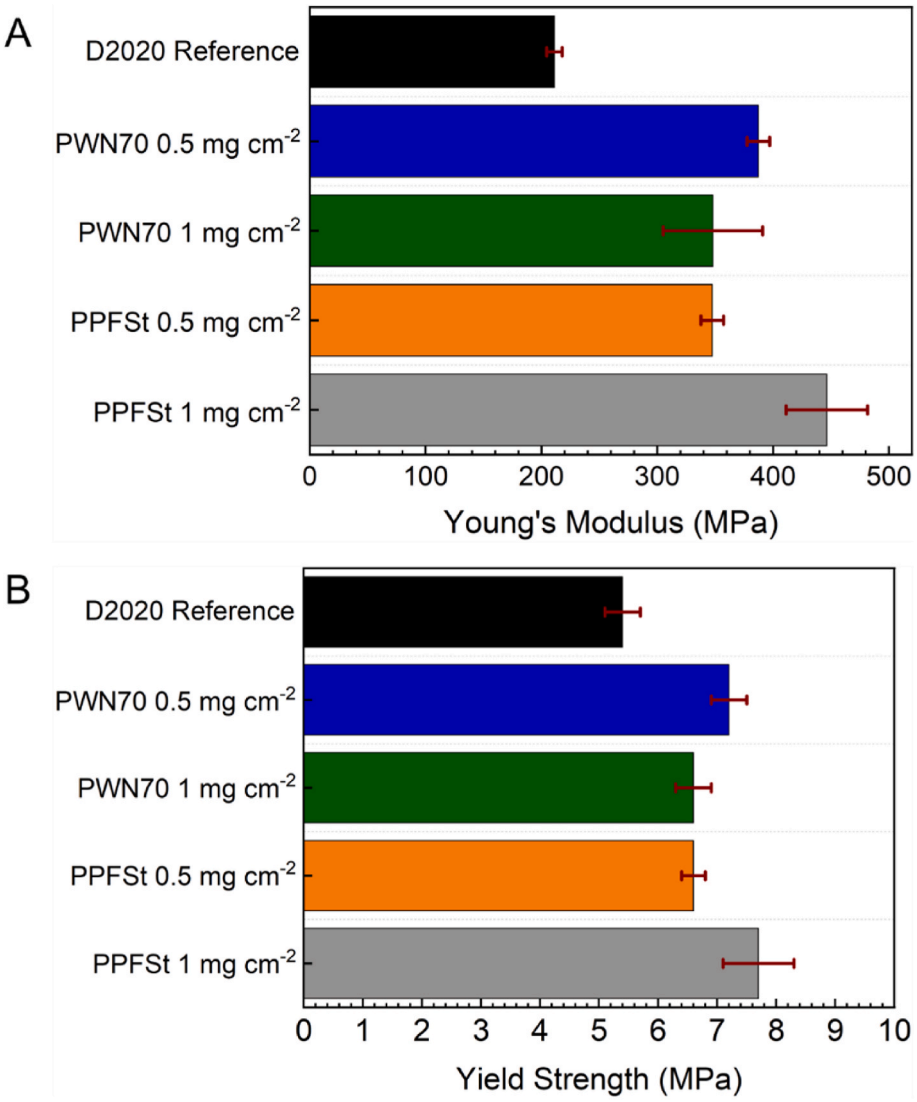

Fig. 7. Mechanical properties of Nafion composite membranes reinforced with different fiber loadings of PWN70 PPFSt nanofibers. A) shows the Young's modulus and B) the yield strength of the membranes. The bars represent the mean of three measurements per each sample, while the error bars represent the standard deviation of these three replicates.

properties of the membranes beyond room temperature (Table S1). In both conditions, the Nafion reference membrane without reinforcement has the lowest Young's Modulus. The Young's Modulus of all membranes is reduced in liquid conditions after equilibrating the membranes in water. The membrane with hydrophobic PPFSt fibers maintains the highest Young's Modulus, whereas the membranes with hydrophilic PWN70 and without reinforcement show a drastic reduction in the Young's Modulus. Nonetheless, even in this maximum hydration case, the PWN70/Nafion composite outperformed non-reinforced Nafion by 39%.

3.3. Fuel cell performance

Fuel cell tests were conducted to analyze the performance of MEAs with the composite membranes. In Fig. 8A, the polarization results show that the MEAs assembled with the conductive PWN70 fiber-reinforced membranes delivered a similar peak power density compared to the reference MEA, with around 650 mW cm^{-2} for both fiber loadings. On the other hand, the MEAs with the PPFSt fiber-reinforced membranes revealed a reduced performance. The effect scales with fiber loading: The MEA with PPFSt fiber composite membranes with a loading of 0.5 mg cm^{-2} resulted in a minor peak power density reduction to approximately 625 mW cm^{-2} (4% reduction) but the samples with a fiber loading of 1.0 mg cm^{-2} showed a larger decrease in peak power density to 564 mW cm^{-2} (13% reduction).

Fig. 8B depicts the HFR as a function of the current density of the MEAs. In the ohmic region (~250–1250 mA cm^{-2}) of the polarization curve, the reference MEA showed an average HFR of approximately 53–57 mΩ cm^2. The HFR of the composite membranes reinforced with conductive PWN70 fibers was similar (55–60 mΩ cm^2), which is in agreement with the polarization data provided in Fig. 8A. The minor increase by up to 3 mΩ cm^2 for the PWN70 fiber-reinforced MEAs can be attributed to the slightly lower proton conductivity of PWN70 compared to Nafion [26] or to interfacial resistances between the two polymers. For the membranes reinforced with non-conductive PPFSt, the HFR increased significantly to around 70 and 85 mΩ cm^2 and scaled with the fiber loading of the membranes. This phenomenon can be attributed to the pure mechanical reinforcement of the non-conductive fiber meshes, which cannot support proton conduction and therefore deteriorate the overall conductivity of the membranes [20]. The HFR-free polarization data (Fig. 8C) shows that the increased HFR is the main reason for the reduction in performance for MEAs assembled with the non-conductive

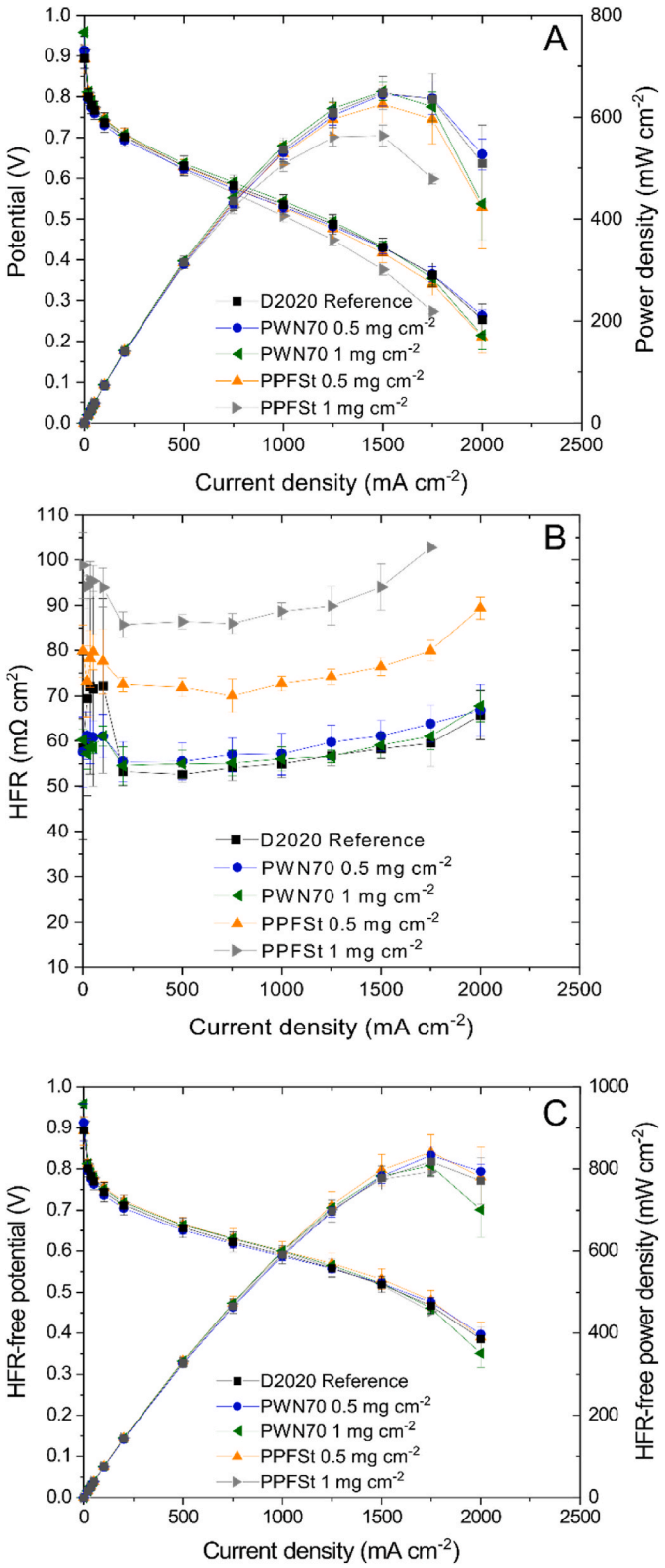

Fig. 8. Polarization data (A), high frequency resistance (HFR) data over current density (B), and HFR-free polarization data of the MEAs with composite membranes (C). The data were acquired at 80 °C, 95% relative humidity, atmospheric pressure, 0.25 l min^{-2} H_2, and 0.75 l min^{-2} air. The data points are the mean of 3 measured MEAs per membrane type, and the error bars indicate the standard deviation of these three repetitions per sample type.

fiber-reinforced membranes since all MEAs perform similarly after the HFR-correction. Thus, the performance loss of the PPFSt-containing MEAs can be attributed to a lower proton conductivity of the PPFSt-reinforced membranes. The proton conductivity is correlated to the IEC, which is presented in Table S2. PWN70 contains phosphonic acid groups, whereas PPFSt has no ionic groups. Consequently, the IEC of PWN70/Nafion membranes is improved compared to Nafion D2020, whereas it is decreased when reinforced with PPFSt fibers. Further, the proton conductivity of all membranes was calculated from the HFR values of the fuel cell tests (Fig. S3 and Table S3) and experimentally determined at room temperature for all three types of membranes (Table S4), which confirms the observed HFR-trends (Fig. 8B). Additionally, we determined the temperature-dependent proton conductivity for the reference and the PWN70 fiber-reinforced MEAs (Table S3), which both showed the expected trends of increasing conductivity with increasing temperature.

The Tafel analysis of all sample types can be seen in the supporting information (Fig. S4) and shows very similar results for all samples. The similar range of Tafel slopes for the 3 repetitions of all MEA types indicates a good comparability between the specimens and rules out significant poisoning of electrodes. However, it is noteworthy that the postprocessing steps of the composite membranes (Fig. 2) are needed to prevent electrode poisoning, which is probably caused by remnants of the solvents used during electrospinning.

Fig. 9 shows the LSV measurements of the different MEAs at atmospheric pressure and at 1.5 bar absolute pressure. The measurements were additionally conducted at 1.5 bar absolute pressure to evaluate the trend at higher pressures, which generally results in an increased hydrogen crossover. The current density measured in the LSV setup corresponds to the H_2 crossover at those conditions. For both pressure settings, a reduction in hydrogen crossover can be observed for the PWN70 fiber-reinforced membranes, whereas the PPFSt fiber-reinforcement did not alter the hydrogen crossover compared to the non-reinforced reference membrane. Table 1 lists the crossover current densities for the different samples, which shows that PWN70 fiber-reinforcements resulted in a H_2 crossover reduction by 37–40% for atmospheric pressure and by 25–30% for 1.5 bar absolute pressure. Notably, this effect did not scale with fiber loading since both PWN70-reinforced composite membranes resulted in a similar crossover reduction.

Both the protonic conductivity and the hydrogen diffusivity rely on water channels in the phase-separated membrane polymer Nafion [45]. Since PPFSt fibers are non-conductive for protons, the increased HFR of the PPFSt-fiber-reinforced membranes compared to the non-reinforced Nafion reference can be explained by an increased resistivity for protons, which can only be transported through the Nafion phase. Additionally, the Raman analysis (Fig. 6) shows the hydrophobic nature of the PPFSt fibers, which likely leads to a poor interface with the Nafion matrix. The SEM images (Fig. 5) support this observation since they revealed a delamination between fiber and matrix, which did not occur for PWN70-reinforced membranes. The poor interaction of PPFSt with Nafion can be attributed to the different molecular structures – aromatic and completely hydrophobic (PPFSt) versus perfluorinated, partially hydrophilic, and partially hydrophobic (Nafion). The LSV measurements show that the PPFSt fiber reinforcement did not reduce the hydrogen crossover. A possible explanation for this result is a diffusion pathway through water reservoirs in the poorly connected interface between PPFSt fibers, and the host matrix, or through damages in the nanophase-separated structure within the matrix polymer. Since PPFSt does not take up water, but Nafion swells and shrinks upon (de)hydration during operation within the PEMFC, it is likely that the interface between PPFSt fibers and the host matrix deteriorates and damages to the matrix structure occur [25]. Therefore, water could occupy potential voids within the matrix or between the fiber/matrix interface. This phenomenon could explain the reduced proton conductivity due to the non-conductive fibers and the unaltered hydrogen diffusion through the

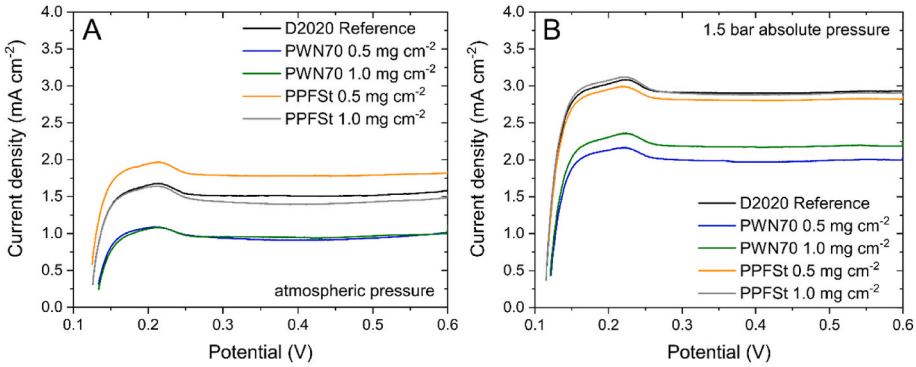

Fig. 9. LSV data of the reference MEAs and the composite MEAs at atmospheric pressure (A) and 1.5 bar absolute pressure (B). Provided is the mean of three independent repetitions per membrane type. The LSV measurements were performed at 80 °C, 95% RH, 0.2 l min^{-2} H_2 in the anode compartment, 0.2 l min^{-2} N_2 in the cathode compartment. The measured current density is proportional to the H_2 crossover. (The individual measurements per MEA type are provided in Fig. S5).

Table 1
Hydrogen crossover current densities acquired by LSV measurements of MEAs assembled with PWN70/PPFSt fiber-reinforced membranes and the reference MEA at atmospheric pressure and at 1.5 bar absolute pressure.

	D2020 Reference/*mA cm*$^{-2}$	PWN70 0.5 mg cm^{-2}/*mA cm*$^{-2}$	PWN70 1.0 mg cm^{-2}/*mA cm*$^{-2}$	PPFSt 0.5 mg cm^{-2}/*mA cm*$^{-2}$	PPFSt 1.0 mg cm^{-2}/*mA cm*$^{-2}$
Atm (1 bar_{abs})	1.51 ± 0.36	0.91 ± 0.19	0.95 ± 0.12	1.78 ± 0.28	1.40 ± 0.15
1.5 bar_{abs}	2.90 ± 0.32	1.97 ± 0.23	2.17 ± 0.30	2.80 ± 0.75	2.88 ± 0.19

liquid phase. Notably, similar results were also observed in the comparison of proton-conductive sulfonated poly(ether ketone) fiber-reinforced membranes and non-conductive poly(vinylidene fluoride-*co*-hexafluoropropylene) fiber-reinforced membranes [20]. Swelling experiments were conducted to further investigate the described behavior (Fig. S6). Both fiber-reinforced membranes show an increased water uptake compared to the reference, which can be explained by the higher water uptake of PWN70 and the hypothesized water-filled voids between PPFSt fibers and the Nafion matrix.

The phosphonation of PPFSt leads to an improved interface compatibility between fibers and matrix, as seen in the SEM images (Fig. 5). We assume that the PWN70 fibers have a lower diffusivity for hydrogen than Nafion, which explains the lower crossover of PWN70-reinforced membranes compared to non-reinforced Nafion. As a consequence, the reinforcement with PWN70 fibers likely increases the tortuosity of the composite membrane for hydrogen diffusion, which predominantly occurs through the Nafion matrix. While hydrogen molecules are decelerated by the increased tortuosity, the proton conductivity is still provided via PWN70, because of its high phosphonation degree. Thus, the resistivity of PWN70-reinforced membranes remains similar compared to the reference Nafion, as it can be observed in the HFR data of the MEAs (Fig. 8B). Thus, the reinforcement of membranes with PWN70 fibers improves the hydrogen-blocking abilities of the composite membrane while at the same time maintaining its performance compared to the reference.

4. Conclusions and outlook

In this study, we showed for the first time the successful implementation of a phosphonated polymer-based electrospun fiber mesh into a PEM. The Nafion composite membranes containing PWN70 nanofibers demonstrated a better fiber-matrix interface than the composite membranes reinforced by unmodified PPFSt and outperformed reference membranes without reinforcement in terms of mechanical properties and hydrogen crossover reduction.

The presence of proton conductive PWN70 nanofibers in composite membranes for PEMFC application showed that the fuel cell performance was maintained in the range of a reference MEA assembled with Nafion, while the hydrogen crossover was reduced significantly. Also, we found that both effects can be observed at lower and higher fiber loadings. Thus, PWN fiber-based reinforcements are a promising means to improve the mechanical stability of PFSA membranes. Notably, the effects did not scale with fiber loading of PWN70 in the composite membrane, which hints toward a probably application-specific ideal fiber mesh density: Young's modulus and yield strength of the composite membrane with higher PWN70 loading (1 mg cm^{-2}) were lower than for the lower fiber loading (0.5 mg cm^{-2}) when testing at ambient conditions. Synergistically, PWN is more temperature-resistant than Nafion, which harbors the potential to apply composite membranes of PWN-reinforced PFSAs in dry and elevated temperature operating conditions. On the other hand, a membrane reinforcement with fibers electrospun from the same polymer but without phosphonation (PPFSt) resulted only in improved mechanical properties, but not in advantages for the PEMFC application: The proton conductivity decreased with increasing fiber loading, and no suppression of gas crossover could be detected.

In summary, we could show that the phosphonated polymer PWN is an effective means to produce composite membranes for PEMFCs with superior mechanical properties and lower fuel crossover than standard PFSA membranes. The combination of phosphonated and sulfonated polymers is a promising strategy to engineer high-performance proton conducting solid polymer electrolytes.

In future work, a parameter study on the effect of fiber loading within the membrane onto the cell performance in dependence of temperature and relative humidity will be performed to investigate the effect of a phosphonated reinforcement layer onto PEMFC operation in dry conditions. Moreover, further studies are planned where composite membranes comprising other combinations of proton-conductive fiber mats with different matrix ionomers will be synthesized and tested in low-temperature fuel cells and other electrochemical applications such as PEM water electrolysis and redox-flow batteries.

CRediT author statement

Muhammad Solihul Mu'min: Conceptualization, methodology, validation, formal analysis, investigation, data curation, writing – original draft, writing – review and editing, visualization. Miriam Komma: Conceptualization, methodology, validation, formal analysis,

investigation, data curation, writing – original draft, writing – review and editing, visualization. Dunia Abbas: validation, methodology, data curation, writing – original draft, writing – review and editing, visualization. Maximilian Wagner: validation, formal analysis, investigation, data curation, writing – original draft, writing – review and editing, visualization. Anja Krieger: validation, formal analysis, investigation, data curation, writing – original draft, writing – review and editing, visualization. Simon Thiele: Conceptualization, methodology, writing – review and editing, supervision, project administration, funding acquisition. Thomas Böhm: Conceptualization, methodology, software, formal analysis, data curation, writing – original draft, writing – review and editing, visualization, supervision, project administration. Jochen Kerres: Conceptualization; methodology, writing – original draft, writing – review and editing, supervision, project administration.

Declaration of competing interest

The authors declare that they have no known competing financial interests or personal relationships that could have appeared to influence the work reported in this paper.

Data availability

Data will be made available on request.

Acknowledgments

The authors gratefully acknowledge financial support from the German Federal Ministry of Education and Research BMBF within the project POWERMEM with a grant number 03EW0012A. In addition, Mr. Mu'min would like to thank the Indonesia Endowment Fund for Education (LPDP) for their support (October 2017–March 2022).

Appendix A. Supplementary data

Supplementary data to this article can be found online at https://doi.org/10.1016/j.memsci.2023.121915.

References

[1] A. Kusoglu, A.Z. Weber, New insights into perfluorinated sulfonic-acid ionomers, Chem. Rev. 117 (2017) 987–1104.
[2] K.D. Kreuer, On the development of proton conducting polymer membranes for hydrogen and methanol fuel cells, J. Membr. Sci. 185 (2001) 29–39.
[3] C.S. Gittleman, A. Kongkanand, D. Masten, W. Gu, Materials research and development focus areas for low cost automotive proton-exchange membrane fuel cells, Current Opinion in Electrochemistry 18 (2019) 81–89.
[4] X.-Z. Yuan, S. Zhang, H. Wang, J. Wu, J.C. Sun, R. Hiesgen, K.A. Friedrich, M. Schulze, A. Haug, Degradation of a polymer exchange membrane fuel cell stack with Nafion® membranes of different thicknesses: Part I. In situ diagnosis, J. Power Sources 195 (2010) 7594–7599.
[5] Y. Singh, F.P. Orfino, M. Dutta, E. Kjeang, 3D failure analysis of pure mechanical and pure chemical degradation in fuel cell membranes, J. Electrochem. Soc. 164 (2017) F1331–F1341.
[6] X. Huang, R. Solasi, Y. Zou, M. Feshler, K. Reifsnider, D. Condit, S. Burlatsky, T. Madden, Mechanical endurance of polymer electrolyte membrane and PEM fuel cell durability, J. Polym. Sci. B Polym. Phys. 44 (2006) 2346–2357.
[7] M. Breitwieser, C. Klose, A. Hartmann, A. Büchler, M. Klingele, S. Vierrath, R. Zengerle, S. Thiele, Cerium oxide decorated polymer nanofibers as effective membrane reinforcement for durable, high-performance fuel cells, Adv. Energy Mater. 7 (2017), 1602100.
[8] C. Klose, P. Trinke, T. Böhm, B. Bensmann, S. Vierrath, R. Hanke-Rauschenbach, S. Thiele, Membrane interlayer with Pt recombination particles for reduction of the anodic hydrogen content in PEM water electrolysis, J. Electrochem. Soc. 165 (2018) F1271–F1277.
[9] K.R. Yoon, K.A. Lee, S. Jo, S.H. Yook, K.Y. Lee, I.-D. Kim, J.Y. Kim, Mussel-inspired polydopamine-treated reinforced composite membranes with self-supported CeO x radical scavengers for highly stable PEM fuel cells, Adv. Funct. Mater. 29 (2019), 1806929.
[10] Y. Huo, Q. Li, Z. Rui, R. Ding, J. Liu, J. Li, J. Liu, A highly stable reinforced PEM assisted by resveratrol and polydopamine-treated PTFE, J. Membr. Sci. 635 (2021), 119453.
[11] S. Jiang, Y. Chen, G. Duan, C. Mei, A. Greiner, S. Agarwal, Electrospun nanofiber reinforced composites: a review, Polym. Chem. 9 (2018) 2685–2720.
[12] J.B. Ballengee, P.N. Pintauro, Composite fuel cell membranes from dual-nanofiber electrospun mats, Macromolecules 44 (2011) 7307–7314.
[13] S. Mollá, V. Compañ, E. Gimenez, A. Blazquez, I. Urdanpilleta, Novel ultrathin composite membranes of Nafion/PVA for PEMFCs, Int. J. Hydrogen Energy 36 (2011) 9886–9895.
[14] M. Breitwieser, C. Klose, M. Klingele, A. Hartmann, J. Erben, H. Cho, J. Kerres, R. Zengerle, S. Thiele, Simple fabrication of 12 μm thin nanocomposite fuel cell membranes by direct electrospinning and printing, J. Power Sources 337 (2017) 137–144.
[15] S. Giancola, M. Zatoń, Á. Reyes-Carmona, M. Dupont, A. Donnadio, S. Cavaliere, J. Rozière, D.J. Jones, Composite short side chain PFSA membranes for PEM water electrolysis, J. Membr. Sci. 570–571 (2019) 69–76.
[16] T.-L.L. Yu, S.-H. Liu, H.-L. Lin, P.-H. Su, Nafion/PBI nanofiber composite membranes for fuel cells applications, in: ASME 2010 8th International Fuel Cell Science, Engineering and Technology Conference, vol. 2, 2010, pp. 631–639. ASMEDC.
[17] D.K. Sharma, J. Shen, F. Li, Reinforcement of Nafion into polyacrylonitrile (PAN) to fabricate them into nanofiber mats by electrospinning: characterization of enhanced mechanical and adsorption properties, RSC Adv. 4 (2014), 39110.
[18] Y. Yao, L. Ji, Z. Lin, Y. Li, M. Alcoutlabi, H. Hamouda, X. Zhang, Sulfonated polystyrene fiber network-induced hybrid proton exchange membranes, ACS Appl. Mater. Interfaces 3 (2011) 3732–3737.
[19] I. Shabani, M.M. Hasani-Sadrabadi, V. Haddadi-Asl, M. Soleimani, Nanofiber-based polyelectrolytes as novel membranes for fuel cell applications, J. Membr. Sci. 368 (2011) 233–240.
[20] C. Klose, M. Breitwieser, S. Vierrath, M. Klingele, H. Cho, A. Büchler, J. Kerres, S. Thiele, Electrospun sulfonated poly(ether ketone) nanofibers as proton conductive reinforcement for durable Nafion composite membranes, J. Power Sources 361 (2017) 237–242.
[21] X. Li, X. Hao, D. Xu, G. Zhang, S. Zhong, H. Na, D. Wang, Fabrication of sulfonated poly(ether ether ketone ketone) membranes with high proton, J. Mater. Sci. 281 (2006) 1–6.
[22] J. Choi, K.M. Lee, R. Wycisk, P.N. Pintauro, P.T. Mather, Nanofiber network ion-exchange membranes, Macromolecules 41 (2008) 4569–4572.
[23] K.-D. Kreuer, S.J. Paddison, E. Spohr, M. Schuster, Transport in proton conductors for fuel-cell applications: simulations, elementary reactions, and phenomenology, ChemInform 35 (2004).
[24] V. Atanasov, A.S. Lee, E.J. Park, S. Maurya, E.D. Baca, C. Fujimoto, M. Hibbs, I. Matanovic, J. Kerres, Y.S. Kim, Synergistically integrated phosphonated poly (pentafluorostyrene) for fuel cells, Nat. Mater. 20 (2021) 370–377.
[25] V. Atanasov, J. Kerres, Highly phosphonated polypentafluorostyrene, Macromolecules 44 (2011) 6416–6423.
[26] V. Atanasov, A. Oleynikov, J. Xia, S. Lyonnard, J. Kerres, Phosphonic acid functionalized poly(pentafluorostyrene) as polyelectrolyte membrane for fuel cell application, J. Power Sources 343 (2017) 364–372.
[27] F. Arslan, J. Dirsch, M. Wagner, A.T. Freiberg, M. Komma, J. Kerres, S. Thiele, T. Böhm, The influence of intrinsically proton conductive electrode binder materials on HT-PEMFC performance, J. Power Sources 553 (2023), 232297.
[28] V. Atanasov, D. Gudat, B. Ruffmann, J. Kerres, Highly phosphonated polypentafluorostyrene: characterization and blends with polybenzimidazole, Eur. Polym. J. 49 (2013) 3977–3985.
[29] V. Atanasov, M. Bürger, S. Lyonnard, L. Porcar, J. Kerres, Sulfonated poly (pentafluorostyrene): synthesis & characterization, Solid State Ionics 252 (2013) 75–83.
[30] M.F. Ashby, H. Shercliff, D. Cebon, Materials: Engineering, Science, Processing and Design, Butterworth-Heinemann, Amsterdam, 2018.
[31] M. Maier, D. Abbas, M. Komma, M.S. Mu'min, S. Thiele, T. Böhm, A comprehensive study on the ionomer properties of PFSA membranes with confocal Raman microscopy, J. Membr. Sci. 669 (2023), 121244.
[32] M.S. Mu'min, T. Böhm, R. Moroni, R. Zengerle, S. Thiele, S. Vierrath, M. Breitwieser, Local hydration in ionomer composite membranes determined with confocal Raman microscopy, J. Membr. Sci. 585 (2019) 126–135.
[33] K.C. Neyerlin, W. Gu, J. Jorne, A. Clark, H.A. Gasteiger, Cathode catalyst utilization for the ORR in a PEMFC, J. Electrochem. Soc. 154 (2007) B279.
[34] R. Makharia, M.F. Mathias, D.R. Baker, Measurement of catalyst layer electrolyte resistance in PEFCs using electrochemical impedance spectroscopy, J. Electrochem. Soc. 152 (2005) A970.
[35] C.J. Angammana, S.H. Jayaram, Analysis of the effects of solution conductivity on electrospinning process and fiber morphology, IEEE Trans. Ind. Appl. 47 (2011) 1109–1117.
[36] U. Stachewicz, F. Modaresifar, R.J. Bailey, T. Peijs, A.H. Barber, Manufacture of void-free electrospun polymer nanofiber composites with optimized mechanical properties, ACS Appl. Mater. Interfaces 4 (2012) 2577–2582.
[37] S.H. de Almeida, Y. Kawano, Thermal behavior of nafion membranes, J. Therm. Anal. Calorim. 58 (1999) 569–577.
[38] J.E. Hensley, J.D. Way, S.F. Dec, K.D. Abney, The effects of thermal annealing on commercial Nafion® membranes, J. Membr. Sci. 298 (2007) 190–201.
[39] K.H. Lim, A.S. Lee, V. Atanasov, J. Kerres, E.J. Park, S. Adhikari, S. Maurya, L. D. Manriquez, J. Jung, C. Fujimoto, I. Matanovic, J. Jankovic, Z. Hu, H. Jia, Y. S. Kim, Protonated phosphonic acid electrodes for high power heavy-duty vehicle fuel cells, Nat. Energy 7 (2022) 248–259.
[40] C. Pitois, S. Vukmirovic, A. Hult, D. Wiesmann, M. Robertsson, Low-loss passive optical waveguides based on photosensitive poly(pentafluorostyrene- co -glycidyl methacrylate), Macromolecules 32 (1999) 2903–2909.
[41] N.J. Everall, Confocal Raman microscopy: common errors and artefacts, Analyst 135 (2010) 2512–2522.

[42] C.S. Gittleman, F.D. Coms, Y.-H. Lai, Membrane durability, in: Polymer Electrolyte Fuel Cell Degradation, Academic, London, 2011, pp. 15–88.
[43] A.M. Dafalla, F. Jiang, Stresses and their impacts on proton exchange membrane fuel cells: a review, Int. J. Hydrogen Energy 43 (2018) 2327–2348.
[44] E. Bülbül, V. Atanasov, M. Mehlhorn, M. Bürger, A. Chromik, T. Häring, J. Kerres, Highly phosphonated polypentafluorostyrene blended with polybenzimidazole: application in vanadium redox flow battery, J. Membr. Sci. 570–571 (2019) 194–203.
[45] T. Mochizuki, K. Kakinuma, M. Uchida, S. Deki, M. Watanabe, K. Miyatake, Temperature- and humidity-controlled SAXS analysis of proton-conductive ionomer membranes for fuel cells, ChemSusChem 7 (2014) 729–733.